THE JOURNAL OF PHYSICAL CHEMISTRY C

Article

pubs.acs.org/JPCC

Optical Spectra of the Special Au_{144} Gold-Cluster Compounds: Sensitivity to Structure and Symmetry

H.-Ch. Weissker,[†,‡] O. Lopez-Acevedo,[§] R. L. Whetten,[∥] and X. López-Lozano*[,∥]

[†]Aix Marseille Université, CNRS, CINaM UMR 7325, 13288 Marseille, France

[‡]European Theoretical Spectroscopy Facility, [§]Department of Applied Physics, COMP Centre of Excellence, Aalto University, P.O. Box 11100, 00076 Aalto, Finland

[∥]Department of Physics & Astronomy, The University of Texas at San Antonio, One UTSA Circle, San Antonio, Texas 78249-0697, United States

ABSTRACT: This report concerns the remarkable fine structure reported recently in the optical absorption spectrum of the ubiquitous icosahedral $Au_{144}(SR)_{60}$ cluster compounds when measured under cryogenic conditions. The theoretical explanation of the spectrum relied upon an I-symmetrized variant of the conventional Pd_{145}-type structure-model; real-time TDDFT calculations revealed that, in contradistinction to the prior state of knowledge, the spectrum is profoundly structured and rich in quantum-state information.[1] Reported herein is an investigation of the sensitivity of the theoretical electronic absorption spectra of this compound to variations in the structure. Both I-symmetric as well as asymmetric structure-models are considered; having the same core structure and connectivity, these differ in the mutual configurations about the pyramidal S atoms, which produce significant structure differences penetrating into the gold core. As R-groups, both methyl ($R=CH_3$) and hydrogen (R=H) are considered. The effects on the structure and spectra of local optimizations employing different exchange-correlation (xc-) functionals are also considered. The results may be summarized as follows: all computed spectra show a rich fine-structure when computed at a similar level of resolution (~0.16 eV, transform limited); the I-symmetric structure with $R=CH_3$ has more pronounced features than the asymmetric structure with the same rest group. This is consistent with the high degree of symmetry-imposed degeneracy in the electronic states of the former. These spectral differences between the I-symmetric and the unsymmetrical models are reduced when the CH_3 R group is replaced by the smaller R=H. Many other systematic differences are noted. In particular, we show explicitly the differences caused by changing the R group, the exchange-correlation functional in the geometry relaxation, and the charge state. The present study contains clear indications as to what factors need to be well-controlled in order to achieve good agreement with available experiment. They will be useful for understanding ligand effects on the optical characteristics of thiolate-protected (and other) noble-metal clusters in this interesting size-range where the plasmon (LSPR) emerges.

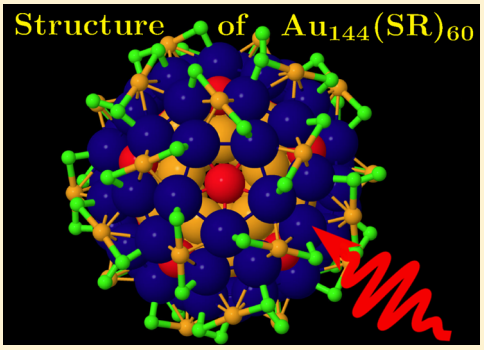

INTRODUCTION

Noble metal clusters are of great importance for the understanding of fundamental physical questions concerning the physics of nanostructured metals. Moreover, monolayer-protected gold clusters have been commercially available for many years ("PeptideGold"[2]) and have been in continuous use in biological and medical investigations over the past decade; applications include bioconjugation chemistry,[3] protein tagging,[2] biomolecule labeling,[4] inhibition of HIV fusion,[5] and growth inhibition of bacteria.[6]

Apart from very small clusters (up to 25 atoms), benchmark results about optical properties are by and large missing. This is particularly true in the intermediate size range where the discrete molecular electronic states develop into the metallic bands of "larger" clusters, while the molecular spectra evolve into smooth spectra. In gold, this is likewise the size where the localized surface-plasmon resonance (LSPR) first emerges.[7,8] For these intermediate sizes, between a few dozens of atoms and ~3 nm in the core diameter, little is known about the "correct" theoretical description. This concerns both the structure and the electronic response: which is the right theoretical description? (In particular, which functional in DFT is appropriate? Are van-der-Waals forces important? Is the spin−orbit coupling important?). On the other hand, there is the equally important question as to what is the correct geometry: how do symmetry-related degeneracies influence the electronic structure and the optical properties? Which geometric details are important and how are they to be taken into account in the simulation of the optical properties?

Special Issue: Current Trends in Clusters and Nanoparticles Conference

Received: December 10, 2014
Revised: February 2, 2015
Published: February 3, 2015

DOI: 10.1021/jp512310x
J. Phys. Chem. C 2015, 119, 11250−11259

On the experimental side, the lack of reproducible benchmark results of the optical properties is mostly due to the fact that experiments had to rely on ensemble measurements where the spectra inevitably suffer substantial inhomogeneous broadening, which can be mainly attributed to the size distribution of the clusters, to impurities, and to disorder in the samples.

By contrast, monolayer-protected clusters form a number of particularly stable cluster compounds (e.g., Au_{25},[9] Au_{55},[10,11] Au_{38},[12] Au_{67},[13] and Au_{144}[14]). Yet even for these systems, limitations in the experimental procedures precluded the measurement of individual spectral structures until recently, even at very low temperatures.[10,15] Progress was made rather recently on the Au_{38} compound[16] and, very recently, on the ubiquitous $Au_{144}(SR)_{60}$[1] which had been reported and believed to be as large as to have necessarily smooth spectra over decades and as recently as in 2013.[7,17]

The $Au_{144}(SR)_{60}$ cluster compound is of particular interest for a number of reasons. Its high stability, reflected in its exceptionally high yield over a broad range of preparative conditions, and its exceptional resistance to degradation, has led to the cluster being synthesized and characterized by a number of groups, and the results are rather reproducible and coherent.[14,18−20] In particular, the optical properties are found to differ but little when different thiolate ligands are employed. In addition, the $Au_{144}(SR)_{60}$ cluster is right in the size region where the LSPR first emerges,[7,8,21] but the rich fine structure of the spectra is not yet covered by the broad LSPR that will dominate the spectra for larger clusters. This is illustrated in Figure 1.

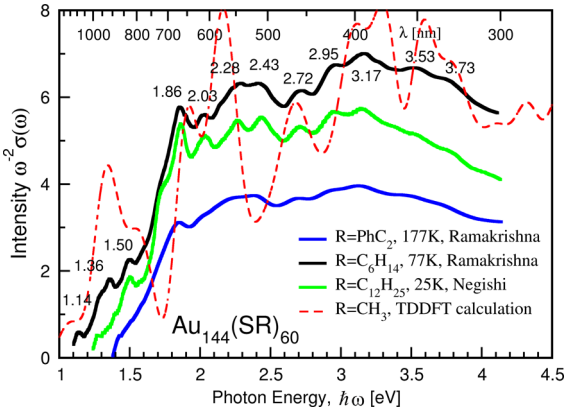

Figure 1. Recent experiments, by different authors and on different samples, showing the high degree of reproducibility of the individual spectral structures of the $Au_{144}(SR)_{60}$. The black and blue lines show data from two measurements on different samples by Ramakrishna et al.[1] The green curve shows data of the recently published measurements by Negishi et al.[45] The fact that the three measurements are done on different samples with different thiolate ligands underlines the reproducibility of the results. The red thin broken line shows the result of the TDDFT calculation.[1]

The determination of the Au_{144} cluster's structure went through many steps. The clusters of this type are all understood to have a core-structure based on the crystal-structure determined for the icosahedral Pd_{145} compound, as reported in 2000 by Tran et al.[22] In 2001, Schaaff et al.[20] reported that the Pd_{145} structure predicts well the peculiar structure factor, determined from X-ray scattering, for the annealed $Au_{144}(SR)_{60}$ clusters.[20] The definite composition (144 Au atoms and 60 thiolate ligands) was indicated in 2008, based on the electrospray mass-spectrometry (ESI-MS) measurements of Chaki et al.[14] This was followed closely by the definitive 2009 reports of Fields-Zinna et al.[23] as well as Qian and Jin.[21] Also reported in 2009 was the first complete structure-model, consistent both with this composition and the staple-motif coordination, by López-Acevedo et al.[24] This essential structure-model (60 thiolate ligands arranged in the so-called staple motifs containing gold adatoms between two sulfur atoms each of which connects the Au core to the thiolate ligands) has provided the basis for all subsequent investigations, including the EXAFS reports of MacDonald et al.[25]

This structure was refined[26] in 2013 to ensure I-symmetry compliance, in order to agree with the NMR measurements,[27] demonstrating the 60-fold symmetry equivalence of the ligand R-groups. These refinements did not change the coordination of the staple motifs. The principal change consists in a symmetry-compliant mutual orientation of the staples. The differences arise only from the conformations (cis vs trans) of the two S-R groups within a staple-motif unit, but these conformations affect the mutual approaches of R-groups in neighboring motifs and appear to introduce significant strain throughout the entire structure, including the metal core. In all the Au_{144} structure-models, the unoccupied site in the Pd_{145} structure, which has been determined unambiguously, is the unique central site. While the overall geometry changes may seem minor, the high symmetry had a strong impact on the electronic structure because of the high degree of degeneracy of the electronic states, in particular of the HOMO. The effect of these changes on the optical response have not yet been investigated in detail until now.

The I-symmetrized and optimized Bahena et al. structure[26] was employed, without any alteration, in the recent report of Weissker et al.[1] For further discussion of this symmetry type, as it applies to the $Au_{144}X_{60}$ (X = SH or Cl), see ref 28.

We emphasize that only the Pd_{145} crystal structure has been determined unambiguously; the others should be regarded as the standard or conventional structure-models, at the present. For that reason, it is important that all available information is used to improve the knowledge about the structure. In particular, the comparison with the recently obtained rich fine structure of the absorption spectra is expected to increase the available knowledge concerning geometrical details. More specifically, the question arises whether the reduced symmetry of the original López-Acevedo et al. structure compared with the full icosahedral symmetry of the symmetrized Bahena et al. structure will result in measurable differences in the optical spectra. This leads to the more general question as to how to describe and study properly the $Au_{144}(SR)_{60}$ cluster compound.

There have been three groups who have, until now, calculated the optical spectra of Au_{144}. Malola et al. have used[7] the structure found by López-Acevedo et al.[24] and reduced the rest group to R=H. The relaxation was done using the LDA. The spectra have been presented using a rather large broadening in order to compare with older experiments.

Barcaro et al.[29] have taken the same structure and symmetrized to D_5 symmetry in order to exploit the reduction of numerical effort due to the use of symmetry in the ADF code.[29] The rest group is R=H, and the geometry optimizations were done using LDA.

Weissker et al. have used[1] the fully symmetric structure of Bahena et al. The structure was taken without change from ref 26, the rest group is R=CH_3, and the relaxation was done using

DOI: 10.1021/jp512310x
J. Phys. Chem. C 2015, 119, 11250−11259

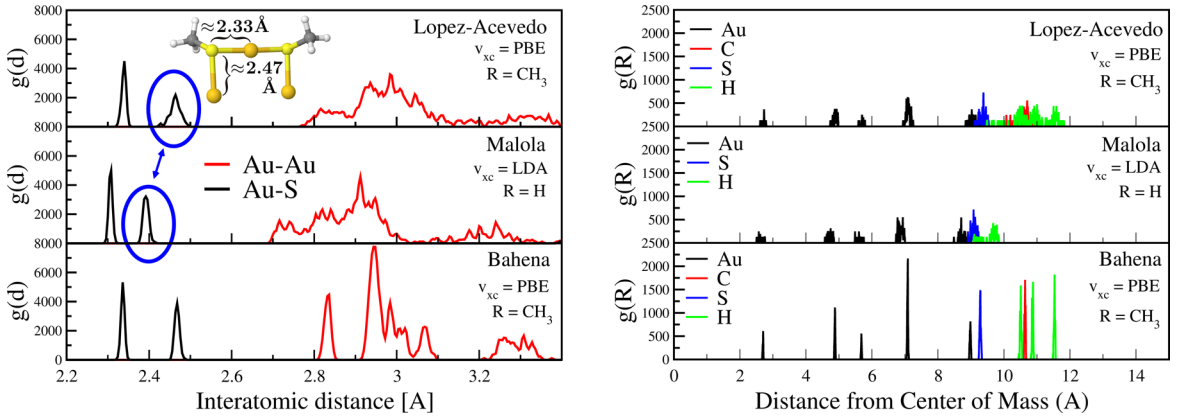

Figure 2. Distribution of interatomic distances (left) and of the radial distances (right) from center (i.e., the center of mass) in the three different cluster structures. The difference between the fully symmetric Bahena et al. structure and the less symmetric versions is quite clear; in particular, the figures show that the distortion extends well into the core, as witnessed by the broadening of the Au−Au bond length distribution compared to the sharp peaks of the fully symmetric structure. We likewise note that the longer Au−S bonds (the side bonds of the staples) are more strongly spread in the López-Acevedo et al. structure with the CH_3 rest group than in the Malola et al. structure where the rest group is reduced to H. The overall shorter distances in the Malola et al. structure are due to the use of the local density approximation (LDA) functional in the relaxation which generally gives shorter bond lengths than the generalized-gradient approximation (GGA).

the PW91 GGA functional and the charge state 2+ to avoid Jahn−Teller distortion.

In general, the agreement between experiment and calculation provides a basis for the assignments of the spectral peaks but remains far from being satisfactory. We have discussed the possible reasons in ref 1.

The direct comparison between theoretical spectra calculated by different groups, using different implementations of time-dependent density-functional theory (TDDFT), remains intricate. In this case, not only the subtle differences between the model structures influence the spectra but also a myriad of technical details. In particular, the proper choice of the basis set or, respectively, the pseudopotential used is of importance, as is the choice of the approximations within DFT and TDDFT (exchange-correlational functional used in the ground-state relaxations; exchange-correlation kernel used in the TDDFT calculation of the spectra).

In the present work, we systematically compare the different structures used and, in particular, discuss the effect of their differences on the optical absorption spectra. To this end, we use exactly the same numerical setup and parameters in all cases which ensures that all differences between the spectra are solely due to the subtle geometry differences. After a short description of the technical approach and of the distinct atomic structures, we present an analysis of the cluster structures and the influence of their differences on the electronic states. After that, we show that the differences between the model structures employed in the recent calculations introduce differences in the spectra that are well-distinguishable on the level of detail of available experiment. In particular, we show the importance of keeping a sufficiently large rest group, CH_3, in the calculations.

METHOD

Theoretical Methods. The optical absorption spectra are calculated by TDDFT using the real-space code octopus.[30,31] Following a ground-state calculation, spectra are calculated using the time-evolution formalism[32] and the PBE exchange-correlation potential.[33] Norm-conserving Troullier-Martins pseudopotentials[34] have been used which, similarly as in our previous work,[1] include the *d* electrons in the valence (11 valence electrons for each Au atom, i.e., ∼ 2,500 active electrons). The spacing of the real-space grid was set to 0.20 Å, the radius of the spheres centered around each atom which make up the calculation domain to 5 Å. The total energy is used to monitor the stability of the propagation. The time step for the propagation was set to 0.00197 fs, the propagation time was 25 fs, and the propagation was carried out by means of the approximated enforced time-reversal symmetry (AETRS) propagator,[35] as implemented in the octopus code. The 25 fs period provides a transform-limited resolution of 40 THz, or ∼0.16 eV, for all the spectra computed and shown in the figures reported herein.

The results of the time-evolution formalism are equivalent to those obtained using the transition-based Casida formalism.[36,37] A comparison of the time-evolution results with a transition-based calculation is shown in the Supporting Information of ref 1 for the thiolate-ligand covered Au_{38} cluster. For a bare Au cluster, a similar comparison is shown in the Supporting Information of ref 38. The good agreement shows likewise that the technical parameters of our calculations are well-controlled.

We consider the following structural models (the name of the first author of the respective relevant publication has been used to designate the structures): (1) López-Acevedo et al. structure, as presented in ref 24. This work has obtained the coordination of the structure. The staple motifs are oriented in an arbitrary manner so that this structure does not have a definite symmetry. The rest group of the thiolate ligands used here is R=CH_3; the relaxation was done using the PBE GGA functional. We employ this structure without any change. (2) Malola et al. structure as employed in the calculations of ref 7. The structure is derived from the López-Acevedo et al. structure; the rest group has been reduced to R=H, probably resulting in a partial symmetrization (see the subsection on the role of the rest group below). The LDA functional was used for the relaxation. We employ this structure without any change. (3) Barcaro et al. as used in ref 29. The structure is likewise derived from the López-Acevedo et al. structure but has been symmetrized to D_5 symmetry. The rest group is R=H. The LDA was employed as the xc-functional in the structural relaxation. (4) Bahena et al. is as presented in ref 26 and used without change in ref 1. The rest group is R=CH_3, and the PW91 GGA[39] was used for the relaxation as well as the charge

DOI: 10.1021/jp512310x
J. Phys. Chem. C 2015, 119, 11250−11259

state 2+ to avoid a Jahn−Teller distortion. We employ this structure without any change.

We furthermore compare to variations of these structures. To study the influence of the xc-functional, we have re-relaxed the Malola et al. structure using PBE for comparison. Moreover, we have reduced the rest groups of the López-Acevedo et al. structure and the Bahena et al. structure, $CH_3 \rightarrow H$ for comparison as discussed in the Results section. These relaxations were done by means of the VASP code[40−42] using density-functional theory (DFT) with the PW91 GGA[39] and with the projector-augmented wave method (PAW).[42] The force tolerance has been set to 0.01 eV/Å.

RESULTS

Comparison of Geometrical and Electronic Structures (Various Models). Using the symmol tool,[43] we have double-checked the symmetries of the different structures. The fully symmetric Bahena et al. structure has indeed icosahedral symmetry *I*. This structure is characterized by (i) the formation of bridging (staple-motif) elements, which is already sufficient to reduce the symmetry from I_h to *I*; (ii) the pyramidization about the thiolate S atom, which need not result in any additional symmetry reduction, provided that all-trans configuration is adopted; and (iii) the complexity or confirmation of the thiolate R-group, which is irrelevant, provided that they are all the same chemical type.

While the fully symmetric Bahena et al. structure has icosahedral symmetry, the orientation of the staples in the two less symmetrical structures, López-Acevedo et al. and Malola et al., destroys the symmetry; no symmetry operations are found.

To quantify the deviation and, in particular, to see if the different orientations of the staples at the surface produce changes in the metallic core as well, we investigate the distribution of atomic bond lengths as well as the radial distribution of the atomic positions from the center of mass of the clusters in Figure 2. Clearly, the distributions of the fully symmetric Bahena et al. structure are more peaked compared to the less symmetric structures where they are more broadened. In particular, the diffuse distributions of the Au−Au bond distances as well as of the radial Au distances from the center show that distortions due to the different orientation of the staples at the surface reach well into the metallic core. Comparing the two models with the full $R = CH_3$, López-Acevedo et al. and Bahena et al., we note that the longer ones of the Au−S bonds (≈ 2.47 Å) show a larger spread in the less symmetric structure. These are the bonds that make the sides of the staples (see Figure 2). For the shorter ones (≈ 2.33 Å) which are the outer bonds of the staple units, the difference is much smaller. Interestingly, this disorder effect due to the lower symmetry depends on the presence of the CH_3 rest groups; in the Malola et al. structure, where CH_3 has been replaced by H compared to the López-Acevedo et al. structure before the relaxation, the spread of the outer Au−S bonds is much smaller. This will be discussed later in the section on the role of the rest group.

The question is now how much these rather subtle differences influence the electronic structure and the optical response. As reported earlier,[28] the fully symmetric Bahena et al. structure results in a high degree of degeneracy of the electronic states. For the neutral cluster, in particular, the HOMO is 5-fold degenerate (times two for spin), but there are only two electrons that would fill these states. The cluster would, therefore, undergo a Jahn−Teller-like distortion so as to lift the degeneracy. The fully symmetric structure, on the other hand, is stable in the charge state 2+. For the lower-symmetry structures, the deviations from the icosahedral symmetry lift the degeneracies entirely.

The electronic density of states shows this effect for the entire electronic structure of the cluster, shown in Figure 3. We

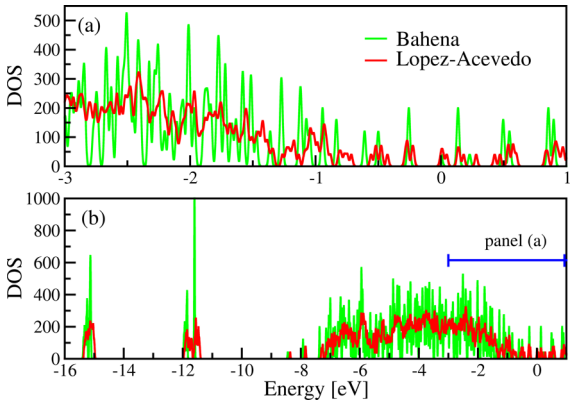

Figure 3. Density of states of the López-Acevedo et al. and the fully symmetric Bahena et al. structures. The upper panel shows a zoom of the region between −3 and 1 eV of the lower panel. The DOS of the Bahena et al. structure is strongly peaked, reflecting the high degree of degeneracy of the electronic structure. By comparison, the DOS of the López-Acevedo et al. structure is smoother, with the peaks broadened due to the breaking of the strict symmetries and the resulting lifting of the degeneracies. Both structures have the rest group $R=CH_3$, whereas the Malola et al. structure is not directly comparable due to its different rest group. Kohn−Sham energies and a broadening of 0.01 eV have been used to calculate the density of states.

compare the fully symmetric Bahena et al. structure and the less symmetric López-Acevedo et al. structure. Both have the rest group $R=CH_3$. (The Malola et al. structure is not directly comparable because here the rest group CH_3 has been replaced by H.) The DOS of the fully symmetric cluster is strongly peaked, attesting to the fact that the degeneracy means that a number of states have exactly the same energy. The DOS of the López-Acevedo et al. structure is broadened, by comparison, the individual contributions are less strongly peaked, which reflects the lifting of the degeneracies. Clearly, the subtle differences between the geometries produce notable differences in the electronic structure.

Sensitivity of the Optical Electronic Spectrum to Structure and Symmetry. The underlying assumption of the use of the different model structures with their subtle differences by the various groups has been that the resulting differences in the optical response should be negligible at the level of available experimental detail. The spectra computed for each of the four extant structure-models are compared in Figure 4, for both the absorption cross section $\sigma(\omega)$ (left panel) and the absorbance, $\sigma(\omega)/\omega^2$ (right panel). The experimental result as published in ref 1 is shown along with the calculations for comparison. We note that the calculation of all the spectra has been carried out here using the same approximations and technical parameters. Therefore, the differences arise solely from the subtle differences between the structures. Moreover, it is clear that the degree of the differences that should be taken into account is dictated by available experiment. As mentioned above, while until recently the spectra of the Au_{144} cluster compound had been considered necessarily smooth and, by and

DOI: 10.1021/jp512310x
J. Phys. Chem. C 2015, 119, 11250−11259

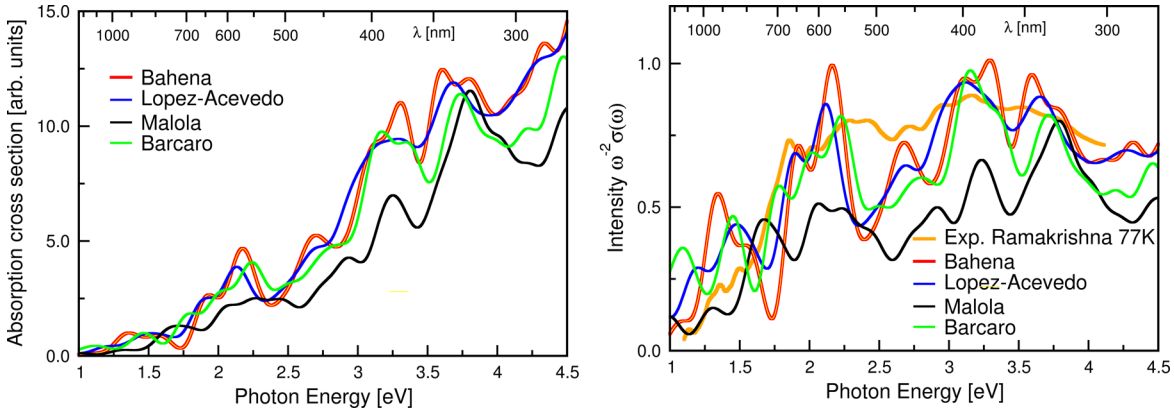

Figure 4. Absorption cross section (left) and absorbance (right) of the different structures. On the right-hand side, we include the data from the experiment of ref 1. Clearly, the differences between the calculated results are non-negligible on the scale of the possible comparison with experiment, which is mainly determined by the distinguishability of the individual peaks in the experiments. The López-Acevedo et al. structure has less structure between 3 and 4 eV than the fully symmetric Bahena et al. structure. There are also strong differences at very low energy (between 1 and 1.75 eV). The Malola et al. structure deviates from the others. In particular below 2 eV, its spectrum is completely different. We show below that part of the difference is due to the use of the LDA functional in the relaxation, unlike for the other structures which have all been relaxed using GGA. Finally, the spectrum of the Barcaro et al. structure is different at low energy. We show below that the differences are partially due to the D_5 symmetrization of this structure.

large, featureless,[1,7,17] it has been shown recently that the spectrum is replete with individual spectral features. The precision with which they can be measured reproducibly determines the precision on which meaningful comparison with (and among) calculations is possible.

We first compare the López-Acevedo et al. structure with the fully symmetric Bahena et al. structure. While the overall shape of the spectra is, of course, not wildly different, there are clear distinctions: the López-Acevedo et al. spectrum is less structured between 3 and 4 eV than the Bahena et al. spectrum which shows two groups of two peaks each (at 3.1 and 3.3 eV and at 3.6 and 3.8 eV). This seems specially important because these spectral structures are in particularly good agreement with experiment.[1] Moreover, the two spectra differ strongly in the low-energy region, between 1.00 and 1.75 eV. The differences are indeed of the order as to allow for conclusions based on the comparison with the experiments.

The structure used by Barcaro et al. results in a spectrum that is likewise in general agreement with that of the Bahena et al. structure as far as the overall shape is concerned. However, also here there is a difference present between 3 and 4 eV, in particular the fact that only one peak is present between 3.5 and 4.0 eV. Moreover, between 1.75 and 2.25 eV where both the López-Acevedo et al. and the Bahena et al. structures produce two peaks, this geometry results in three. We will show below that this is due to the different symmetrization (see Figure 5). Below 1.7 eV, the spectrum is closer to the López-Acevedo et al. than to the Bahena et al. spectrum.

Finally, the Malola et al. structure produces a spectrum that is rather different from either of the others. The main differences, as will be shown below, are due to the use of H atoms in lieu of the bigger rest group CH_3, as well as the use of the LDA xc-functional in the relaxation of the structure.

These comparisons show clearly that the subtle differences of the geometric models used by the different groups lead to differences in the spectra that are non-negligible on the level of the comparison with experiment. We will now investigate in detail the different influences.

Anisotropy. The optical response of the fully symmetric Bahena et al. structure is necessarily isotropic due to the

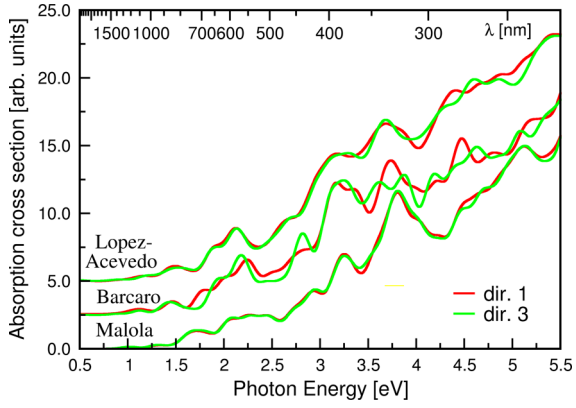

Figure 5. Anisotropy for the three original model structures: shown are the spectra for each of the structures in two different directions. Direction 1 is a 5-fold symmetry axis in all the cases (approximate, for the López-Acevedo et al. and the Malola et al. structures). Although the spectra are somewhat anisotropic, the effect it not very strong. Interestingly, the anisotropy of the López-Acevedo et al. structure is stronger than that of the Maola et al. structure, indicating the importance of the rest group CH_3. The Barcaro et al. structure was symmetrized to D_5 symmetry in order to reduce the numerical effort. The anisotropy demonstrates that this symmetrization is not inconsequential.

symmetry. In order to quantify the anisotropy for the less symmetric structures, we compare in Figure 5 the response in one direction (along a 5-fold axis) with a different direction perpendicular to the first. Both the López-Acevedo et al. structure and the Malola et al. structure derived from it show a low degree of anisotropy. The only real differences are seen above 3 eV, and they are small, although in the case of the López-Acevedo et al. structure, they may contribute to the fact that only one and not two peaks (as for the Bahena et al. structure) are seen between 3.5 and 4.0 eV. The full spectrum is, of course, the average (or, more precisely, the trace of the full tensor). Thus, the anisotropy itself is found to be smaller than the difference to the other structure. Moreover, the Malola et al. structure shows a lower degree of anisotropy. This is probably

DOI: 10.1021/jp512310x
J. Phys. Chem. C 2015, 119, 11250−11259

due to the fact that the CH_3 rest groups have been replaced by H as compared to the other models, see also the subsection on the role of the rest group below.

Finally, we compare with the structure used by Barcaro et al. This cluster, in which D_5 symmetry has been introduced, shows the largest anisotropy of all the considered geometries. Between 1.5 and 2.5 eV, the number of peaks is different in the two directions, and the fine structure above 3.5 eV is also rather different between the directions. The full spectrum is, of course, dependent on these differences. While for the fully I-symmetric structure obtained for the charge state 2+, the D_5 model is not pertinent, it might well be applicable for Jahn−Teller-distorted clusters, depending on the charge stage (e.g., for the neutral cluster).

Influence of Exchange-Correlation Functional. Apart from the connectivity of the geometry and the symmetry, the calculations need to apply certain approximations. First of all, once the geometry is constructed, a local relaxation using static DFT is carried out in all the cases. For this, the choice of the xc-functional is clearly of importance. Unfortunately, there is no systematic improvement going from one choice to the next. Malola et al. and Barcaro et al. have used the LDA functional, while all other structures studied in the present work used a GGA. LDA is known to somewhat underestimate bond distances in general, while the opposite is the case for the GGA. Nonetheless, for pure Au systems, the LDA seems to give slightly better results than the GGA. For the system including the ligands, it would be difficult to make any clear prediction as to what functional is the proper choice. In the following, we study the difference induced by the two different functionals *during the relaxation*. Clearly, we can only discuss the difference, the choice of what is the best functional for the $Au_{144}(SR)_{60}$ cluster compound will have to rely on comparison with experiment.

To this end, we compare the spectrum of the original Malola et al. structure with that of the same structure, relaxed once more but now with the PBE GGA functional. We note that the calculation of the spectra is done in both cases using PBE; the differences in the spectra are solely due to differences in the geometry. The comparison is shown in Figure 6. While the difference is not enormous, there are clearly changes that are relevant for the comparison with the experiment. In particular, between 2.0 and 2.5 eV, the spectra differ seriously. The same is true just above 4 eV where the shoulder of the LDA-relaxed cluster develops into two peaks in the rerelaxation using PBE. This shows clearly that the choice of the functional for the ground-state relaxation is not entirely innocuous. In particular, the differences are not restricted to a simple shift or scaling. Future work should enable detailed choices based on all quantities.

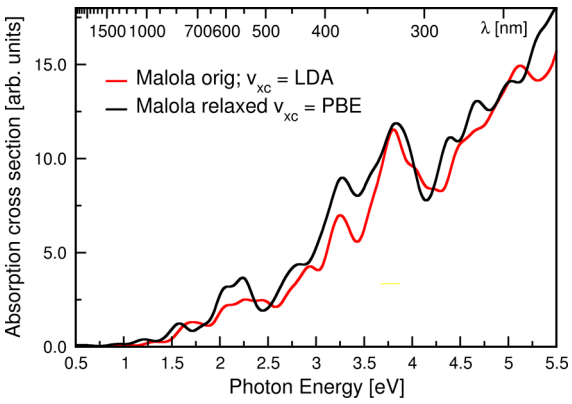

Figure 6. Comparison of different functionals used in the relaxation (note that for the given geometries, both spectra are calculated with the same numerical setup and the PBE functional). Clearly, the differences are rather large on the scale determined by the comparison with experiment.

Role of the Rest Group: R=H vs R=CH_3. Another important choice for the modeling of $Au_{144}(SR)_{60}$ is that of the rest group. Experiment appears to be rather insensitive to the precise nature of the ligand rest group.[1,44] In the calculations, this has been exploited by cutting down the SR ligands to the minimum necessary. The compromise is between completeness and numerical effort. While the real-world examples contain different, typically rather long thiolate ligands, the huge numerical effort necessitates the reduction as far as possible without losing the essential features of the results.

While most of the studies have considered only the smallest possible choice R=H (i.e., the entire rest group is presented by just one H atom), we have in the past considered the choice of R=CH_3, in particular in the calculations reported in ref 1. To study the difference, we compare the original spectrum of the Bahena et al. structure with R=CH_3 to the same structure after the replacement of CH_3 by H and subsequent relaxation. The spectra in Figure 7 show that the replacement is not without consequence. While below 2.5 eV, the effect is limited to a slight energetic shift, the spectra deviate strongly above 3 eV. In other words, the CH_3 groups cannot be replaced by just H for proper modeling. Future work will have to determine the mechanism of the changes and, in particular, how the presence of the ligands and, more in general, the polarizable matrix influences the spectra. Mechanisms can be charge transfer, general changes in the electronic structure, or simply the presence of the polarizable surroundings, including both ligands and the matrix material.

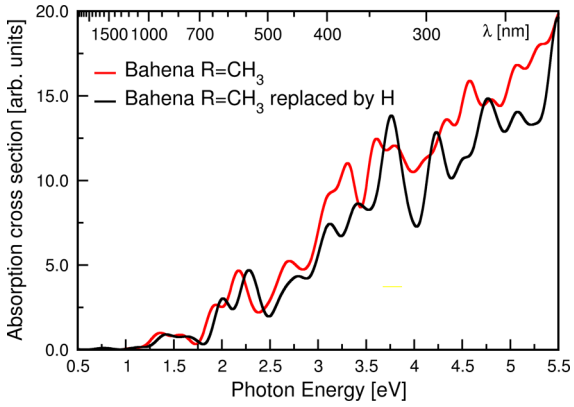

Figure 7. Influence of the ligand rest group in the calculation using the fully symmetric Bahena et al. structure. Red is the original result with R=CH_3 as published in ref 1, while for the black curve, CH_3 has been replaced by H and the structure has been relaxed again. Both relaxations are done using GGA, as is the calculation of the spectra. For the low-energy part, the difference consists at best in a tiny shift, while at higher energies, above 3 eV, the differences are substantial. The comparison shows that the adequate consideration of the rest group is important, and the modeling using R=H is apparently not sufficient.

DOI: 10.1021/jp512310x
J. Phys. Chem. C 2015, 119, 11250−11259

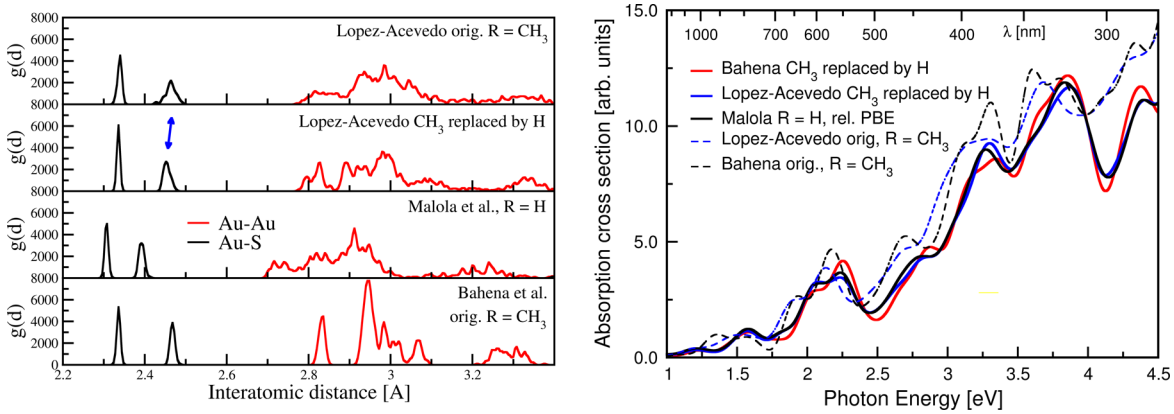

Figure 8. Importance of the rest group, R=CH_3 vs R=H, for the interatomic distances (left) and the spectra (right). The less symmetric structures show a broader bond length distribution. This is particularly visible for the longer Au−S bonds (≈ 2.47 Å, side of the staples, cf., Figure 2). The replacement of R=CH_3 by R=H and subsequent relaxation somewhat reduce the width of the distribution. This is likewise the case in the Malola et al. structure. The resulting spectra, shown on the right-hand side, are very similar between the different geometries with R=H. These spectra are compared with those of the model structures using R=CH_3 (the same already shown in Figure 4) which are, as shown above, rather different both from the calculations with R=H and between each other. This underlines the importance of taking into account (at least) the rest group CH_3.

While from these findings we cannot conclude that CH_3 is entirely sufficient for the modeling, we can conclude that the choice of the mere H atom as applied in a number of published investigations is not sufficient if comparability with the available experiments is sought.

Having shown the importance of the CH_3 groups, we conclude the present study by showing that these rest groups are also important for the distinction between the fully symmetric structure and the less symmetric ones. As already shown in Figure 2, the spread of the length of the longer Au−S bonds (i.e., the side bonds on the staple motives) is different between the López-Acevedo et al. structure and the Malola et al. structure which has been derived from it by replacing CH_3 by H. While in the López-Acevedo et al. structure, these bonds show a spread that is clearly visible in Figure 2, they are clearly less spread in the Malola et al. structure where they appear not very different from the fully symmetric Bahena et al. geometry. (The fact that they are slightly shorter is due to the use of LDA in the relaxation.)

We study once more the distribution of the interatomic distances. It was already found in Figure 2 that the distribution of the side Au−S bonds of the staple motives are much broader than in the case of the Malola et al. model that used R=H from the start. In Figure 8, we see that the simple procedure of replacing CH_3 by H along the direction of the Au−S bond and relaxing once more reduces the width of the distribution of these bonds. Likewise, the distribution of the outer Au−S bonds of the staples gets slightly narrower, although this effect is not very strong. It can be concluded that the replacement of the rest group, H for CH_3, reduces the disorder and strain in the staple motives. In the case of the Malola et al. structure, this was obtained from the start. We can now compare the effect on the spectra. To this end, we also carry out the replacement $CH_3 \rightarrow$ H for the Bahena et al. structure, including relaxation. Interestingly, the spectra obtained for the three structures with R=H are very similar, even though the less symmetrical structures are somewhat distorted even in the core as shown by the Au−Au bond length distribution. However, this agreement is somewhat fortuitous, as the spectra differ seriously from those calculated using the rest group CH_3, which differ appreciably between the fully symmetric Bahena et al. structure and the less symmetric López-Acevedo et al. structure as shown above. This is likewise shown in Figure 8 where we include the López-Acevedo et al. and Bahena et al. structures for direct comparison.

These findings emphasize once more that the choice of the rest group in the calculation is indeed important. The distinguishability based on the optical spectra between the fully symmetric Bahena et al. structure and the less symmetric clusters gets lost when the rest group is simplified too much (in this case, to H only).

Influence of the Charge State. The experimental determination and control of the charge state is difficult; the implicit assumption of a homogeneous charge-neutral cluster distribution in the low-temperature measurements may be unwarranted. For the calculations, the role of the charge state is 2-fold. On the one hand, as described above, Jahn−Teller-like distortions may reduce the symmetry depending on the degeneracy of the HOMO, which in turn depends on the charge state. On the other hand, for a given geometry, the charge state will likewise influence the spectrum simply because the electronic system changes. Here, we study this effect for the fully symmetric Bahena et al. structure for fixed geometry as determined[26] in the charge state 2+. The resulting spectra are shown in Figure 9 for the neutral cluster and the doubly

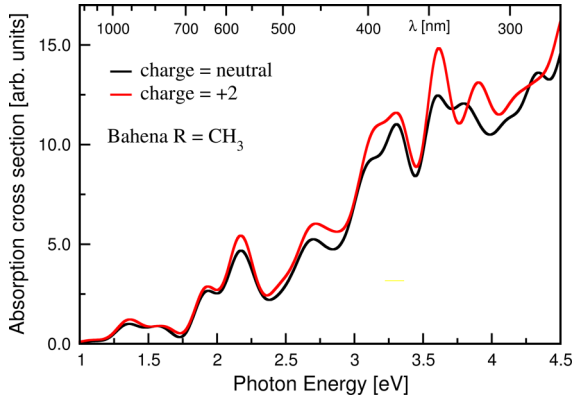

Figure 9. Dependence of the spectra on the charge state. We show the calculations for fixed geometry as determined for the charge state 2+ of the Bahena et al. fully symmetric cluster.

DOI: 10.1021/jp512310x
J. Phys. Chem. C 2015, 119, 11250−11259

charged cluster. It appears that the change is minor, in particular below 3 eV. Above, the changes are slightly larger, although all the structures are still there. Only the peak just below 4 eV is somewhat shifted and smeared or effectively smoothed out. While these changes are not enormous, they are large enough as to have to be taken into account when precise comparison with experiment is needed. Naturally, if the Jahn−Teller-like distortions are taken into account, the changes would be bigger. However, this concerns only highly symmetric structures with a high degree of degeneracy of the electronic states.

CONCLUSIONS

The spectral structures found in recent measurements of the $Au_{144}(SR)_{60}$ cluster compound are very reproducible, which holds even for different thiolate ligand rest groups. The details of these spectral structures define the level of detail up to which the calculations are meaningfully comparable with experiments, which shows 13 peaks/shoulders between 1 and 4 eV. This comparison with experiment imposes likewise the magnitude of differences between calculated spectra that should be considered meaningfully distinguishable.

The different model structures used by different groups have all the same basic structure type, namely the one in which 30 bridging [RS-Au-SR] units attach radially to 60 Au surface atoms in the familiar "staple-motif" configuration, and the metal-atom sites are arranged similarly to those in the totally determined Pd_{145} structures of icosahedral symmetry (i.e., within concentric shells of [1]-12-(30 + 12)-(60 + 30) sites) and with 60 equivalent ligands (thiolates in place of carbonyls C═O). The differences in the structures considered herein are considered to arise only from the conformations (cis vs trans) of the two S-R groups within a staple-motif unit, but these conformations affect the mutual approaches of R-groups in neighboring motifs and appear to introduce significant strain throughout the entire structure, including the metal core. The mutual orientation of the staple motives at the surface, which in the seminal earlier work lead to a surface disorder, was later improved upon by symmetrizing the structure to full icosahedral geometry consistent with available NMR experiments. We find that the distortions resulting from the orientation of the staples extend well into the metallic Au core. The distortions compared to the fully symmetric Bahena et al. structure lift the degeneracy of the HOMO and, in general, lead to a much less strongly peaked density of states.

Detailed comparison of the spectra obtained using an identical numerical procedure in each of the cases shows that the subtle geometry differences between the model structures result in differences that are clearly distinguishible on the order of detail dictated by comparison with experiment. While the anisotropy of the less symmetric structures is rather small, the differences between the resulting complete spectra are non-negligible. We find that the xc-functional used in the relaxation of the structure induces serious differences which will need to be controlled for precise comparison with the experiment. Moreover, our calculations show that the ligands' rest groups need to be taken into account properly; we used $R=CH_3$ in our calculations. A serious difference is found upon replacement of CH_3 by H, as it has been used in a number of other calculations. While this does not necessarily mean that CH_3 is sufficient for the modeling, we can clearly conclude that the reduction of the rest group to H only is too drastic as to enable precise results.

Interestingly, the replacement $CH_3 \rightarrow$ H does not only change the spectra. We found that in relaxation after the replacement, the resulting structures become more symmetric, as seen by the somewhat reduced spread of, in particular, the Au−S bond lengths. Subsequently, these slightly more symmetric structures produce spectra that are very similar but different from those obtained for the more complete models using $R=CH_3$ (i.e., the López-Acevedo et al. and Bahena et al. structures).

For the time being, the differences between the structures and the different ways of modeling (rest group, symmetry, and xc-functional) do not allow for definite conclusions. The agreement between available experiment and theory is far from being satisfactory. However, the present results show which quantities and which influences need to be precisely controlled in order to reach meaningful comparison. The exchange-correlation approximation used in the calculation of the spectra, not treated here, will likewise be important.

The clear and reproducible experiments show that the $Au_{144}(SR)_{60}$ cluster compound is far from being a homogeneous metal cluster. The beauty of these recent results is that they enable the precise comparison between theoretical predictions and experimental results. In future calculations, the influences discussed in the present work clearly need to be taken into account. Apart from providing the basis for the comparison of subtle geometric differences, this will enable clear conclusions concerning the fundamental physical description of intermediate-sized noble metal clusters. It is crucial here to appreciate that the electronic structure methods, including the optical response calculations, are capable of describing correctly the transition from nonplasmonic (either smeared-out spectral functions or richly detailed fine-structure) to collective or plasmonic response, as has been adequately documented for related systems (ligand free clusters of various sizes and shapes including those comparable to those of the Au_{144} system).[7,8,21,45]

Certainly, it remains a possibility that there is some serious inadequacy remaining in the structure model(s), the sensitivity to which is a major theme of the work. In the case of the smaller homologues (thiolate-protected gold clusters) where the structure has been determined and high-level electronic-structure theory has been applied, the agreement is now considered quite satisfactory. These include the well-established cases of the $Au_{25}(SR)_{18}$[9] and the $Au_{38}(SR)_{24}$[12] systems. The supplementary file of ref 1 shows a comparison between the low-temperature spectrum of the latter system and the spectrum computed theoretically starting from the atomic coordinates (crystallographically determined), and the agreement found is sufficient in that case to establish the appropriateness of the methods (and other assumptions regarding crystal vs solution phase structure).

AUTHOR INFORMATION

Corresponding Author

*E-mail: Xochitl.LopezLozano@utsa.edu.

Notes

The authors declare no competing financial interest.

ACKNOWLEDGMENTS

We thank Alessandro Fortunelli and Hannu Häkkinen for providing us with the coordinates used in their respective works, as well as for fruitful discussions. X.L.L. acknowledges

DOI: 10.1021/jp512310x
J. Phys. Chem. C 2015, 119, 11250−11259

funding from NSF-DMR-1103730 and NSF-PREM DMR-0934218. This work received computational support from the Computational System Biology Core, funded by the National Institute on Minority Health and Health Disparities (G12MD007591) from the National Institute of Health, as well as the Texas Advanced Computing Center (TACC) at the University of Texas at Austin. Part of the calculations were done using HPC resources from GENCI-IDRIS (Grant 2014-096829). Moreover, we acknowledge support from the European Union through the COST Action MP0903. R.L.W. acknowledge funding from the Robert A. Welch Foundation Grant AX1857. H.C.W. acknowledges support from the French National Research Agency (Agence Nationale de Recherche, ANR) in the frame of the project "FIT SPRINGS", ANR-14-CE08-0009.

REFERENCES

(1) Weissker, H.-C.; Escobar, H. B.; Thanthirige, V. D.; Kwak, K.; Lee, D.; Ramakrishna, G.; Whetten, R.; López-Lozano, X. Information on Quantum States Pervades the Visible Spectrum of the Ubiquitous Au_{144} Gold Nanocluster. *Nat. Commun.* **2014**, *5*, 1−8.

(2) Hainfeld, J. F.; Liu, W.; Halsey, C. M.; Freimuth, P.; Powell, R. D. Ni−NTA−Gold Clusters Target His-Tagged Proteins. *J. Struct. Biol.* **1999**, *127*, 185−198.

(3) Ackerson, C. J.; Jadzinsky, P. D.; Sexton, J. Z.; Bushnell, D. A.; Kornberg, R. D. Synthesis and Bioconjugation of 2 and 3 nm-Diameter Gold Nanoparticles. *Bioconjugate Chem.* **2010**, *21*, 214−218.

(4) Ackerson, C. J.; Powell, R. D.; Hainfeld, J. F. In *Cryo-EM Part A Sample Preparation and Data Collection*; Jensen, G. J., Ed.; Methods in Enzymology; Academic Press: Waltham, 2010; Vol. *481*; pp 195 − 230.

(5) Bowman, M.-C.; Ballard, T. E.; Ackerson, C. J.; Feldheim, D. L.; Margolis, D. M.; Melander, C. Inhibition of HIV Fusion with Multivalent Gold Nanoparticles. *J. Am. Chem. Soc.* **2008**, *130*, 6896−6897.

(6) Bresee, J.; Maier, K. E.; Boncella, A. E.; Melander, C.; Feldheim, D. L. Growth Inhibition of Staphylococcus Aureus by Mixed Monolayer Gold Nanoparticles. *Small* **2011**, *7*, 2027−2031.

(7) Malola, S.; Lehtovaara, L.; Enkovaara, J.; Häkkinen, H. Birth of the Localized Surface Plasmon Resonance in Monolayer-Protected Gold Nanoclusters. *ACS Nano* **2013**, *7*, 10263−10270.

(8) Qian, H.; Zhu, Y.; Jin, R. Atomically Precise Gold Nanocrystal Molecules with Surface Plasmon Resonance. *Proc. Natl. Acad. Sci. U.S.A.* **2012**, *109*, 696−700.

(9) Parker, J. F.; Fields-Zinna, C. A.; Murray, R. W. The Story of a Monodisperse Gold Nanoparticle: $Au_{25}L_{18}$. *Acc. Chem. Res.* **2010**, *43*, 1289−1296.

(10) Fauth, K.; Kreibig, U.; Schmid, G. Optical Properties of Systems Containing Au_{55}-Clusters. *Z. Phys. D: At., Mol. Clusters* **1989**, *12*, 515−520.

(11) Walter, M.; Moseler, M.; Whetten, R. L.; Häkkinen, H. A 58-Electron Superatom-Complex Model for The Magic Phosphine-Protected Gold Clusters (Schmid-gold, Nanogold of 1.4-nm Dimension. *Chem. Sci.* **2011**, *2*, 1583−1587.

(12) Qian, H.; Eckenhoff, W. T.; Zhu, Y.; Pintauer, T.; Jin, R. Total Structure Determination of Thiolate-Protected Au_{38} Nanoparticles. *J. Am. Chem. Soc.* **2010**, *132*, 8280−8281.

(13) Nimmala, P. R.; Yoon, B.; Whetten, R. L.; Landman, U.; Dass, A. $Au_{67}(SR)_{35}$ Nanomolecules: Characteristic Size-Specific Optical, Electrochemical, Structural Properties and First-Principles Theoretical Analysis. *J. Phys. Chem. A* **2013**, *117*, 504−517.

(14) Chaki, N. K.; Negishi, Y.; Tsunoyama, H.; Shichibu, Y.; Tsukuda, T. Ubiquitous 8 and 29 kDa Gold:Alkanethiolate Cluster Compounds: Mass-Spectrometric Determination of Molecular Formulas and Structural Implications. *J. Am. Chem. Soc.* **2008**, *130*, 8608−8610.

(15) Kreibig, U.; Vollmer, M. *Optical Properties of Metal Clusters*; Springer-Verlag: Berlin, Heidelberg, NY, 1995.

(16) Devadas, M. S.; Bairu, S.; Qian, H.; Sinn, E.; Jin, R.; Ramakrishna, G. Temperature-Dependent Optical Absorption Properties of Monolayer-Protected Au_{25} and Au_{38} Clusters. *J. Phys. Chem. Lett.* **2011**, *2*, 2752−2758.

(17) Jin, R. Quantum Sized, Thiolate-Protected Gold Nanoclusters. *Nanoscale* **2010**, *2*, 343−362.

(18) Alvarez, M. M.; Khoury, J. T.; Schaaff, T. G.; Shafigullin, M. N.; Vezmar, I.; Whetten, R. L. Optical Absorption Spectra of Nanocrystal Gold Molecules. *J. Phys. Chem. B* **1997**, *101*, 3706−3712.

(19) Chen, S.; Ingram, R. S.; Hostetler, M. J.; Pietron, J. J.; Murray, R. W.; Schaaff, T. G.; Khoury, J. T.; Alvarez, M. M.; Whetten, R. L. Gold Nanoelectrodes of Varied Size: Transition to Molecule-Like Charging. *Science* **1998**, *280*, 2098−2101.

(20) Schaaff, T. G.; Shafigullin, M. N.; Khoury, J. T.; Vezmar, I.; Whetten, R. L. Properties of a Ubiquitous 29 kDa Au:SR Cluster Compound. *J. Phys. Chem. B* **2001**, *105*, 8785−8796.

(21) Qian, H.; Jin, R. Controlling Nanoparticles with Atomic Precision: The Case of $Au_{144}(SCH_2CH_2Ph)_{60}$. *Nano Lett.* **2009**, *9*, 4083−4087.

(22) Tran, N.; Powell, D.; Dahl, L. Nanosized $Pd_{1455}(CO)_x(PEt_3)_{30}$ Containing a Capped Three-Shell 145-Atom Metal-Core Geometry of Pseudo Icosahedral Symmetry. *Angew. Chem., Int. Ed.* **2000**, *39*, 4121−4125.

(23) Fields-Zinna, C. A.; Sardar, R.; Beasley, C. A.; Murray, R. W. Electrospray Ionization Mass Spectrometry of Intrinsically Cationized Nanoparticles, $[Au_{144/146}(SC_{11}H_{22}N(CH_2CH_2)_3^+)_x(S(CH_2)_5CH_3)_y]^{x+}$. *J. Am. Chem. Soc.* **2009**, *131*, 16266−16271.

(24) Lopez-Acevedo, O.; Akola, J.; Whetten, R. L.; Grönbeck, H.; Häkkinen, H. Structure and Bonding in the Ubiquitous Icosahedral Metallic Gold Cluster $Au_{144}(SR)_{60}$. *J. Phys. Chem. C* **2009**, *113*, 5035−5038.

(25) MacDonald, M. A.; Zhang, P.; Qian, H.; Jin, R. Site-Specific and Size-Dependent Bonding of Compositionally Precise Gold-Thiolate Nanoparticles from X-ray Spectroscopy. *J. Phys. Chem. Lett.* **2010**, *1*, 1821−1825.

(26) Bahena, D.; Bhattarai, N.; Santiago, U.; Tlahuice, A.; Ponce, A.; Bach, S. B. H.; Yoon, B.; Whetten, R. L.; Landman, U.; Jose-Yacaman, M. STEM Electron Diffraction and High-Resolution Images Used in the Determination of the Crystal Structure of the $Au_{144}(SR)_{60}$ Cluster. *J. Phys. Chem. Lett.* **2013**, *4*, 975−981.

(27) Wong, O. A.; Heinecke, C. L.; Simone, A. R.; Whetten, R. L.; Ackerson, C. J. Ligand Symmetry-Equivalence on Thiolate Protected Gold Nanoclusters Determined by NMR Spectroscopy. *Nanoscale* **2012**, *4*, 4099−4102.

(28) Tlahuice-Flores, A.; Black, D. M.; Bach, S. B. H.; Jose-Yacaman, M.; Whetten, R. L. Structure & Bonding of The Gold-Subhalide Cluster I-$Au_{144}Cl_{60}$[z]. *Phys. Chem. Chem. Phys.* **2013**, *15*, 19191−19195.

(29) Barcaro, G.; Sementa, L.; Fortunelli, A.; Stener, M. Comment on "$(Au-Ag)_{144}(SR)_{60}$ Alloy Nanomolecules" by Kumara, C.; Dass, A. *Nanoscale* **2011**, *3*, 3064 DOI: 10.1039/C4NR00514G.

(30) Marques, M. A. L.; Castro, A.; Bertsch, G. F.; Rubio, A. Octopus: A First-Principles Tool for Excited Electron-Ion Dynamics. *Comput. Phys. Commun.* **2003**, *151*, 60−78.

(31) Castro, A.; Marques, M. A. L.; Appel, H.; Oliveira, M.; Rozzi, C.; Andrade, X.; Lorenzen, F.; Gross, E. K. U.; Rubio, A. Octopus: A Tool for The Application of Time-Dependent Density Functional Theory. *Phys. Status Solidi B* **2006**, *243*, 2465−2488.

(32) Yabana, K.; Bertsch, G. F. Time-Dependent Local-Density Approximation in Real Time. *Phys. Rev. B* **1996**, *54*, 4484−4487.

(33) Perdew, J. P.; Burke, K.; Ernzerhof, M. Generalized Gradient Approximation Made Simple. *Phys. Rev. Lett.* **1996**, *77*, 3865−3868.

(34) Troullier, N.; Martins, J. L. Efficient Pseudopotentials for Plane-Wave Calculations. *Phys. Rev. B* **1991**, *43*, 1993−2006.

(35) Castro, A.; Marques, M. A. L.; Rubio, A. Propagators for The Time-Dependent Kohn−Sham Equations. *J. Chem. Phys.* **2004**, *121*, 3425−3433.

DOI: 10.1021/jp512310x
J. Phys. Chem. C 2015, 119, 11250−11259

(36) Casida, M. E. In *Recent Advances in Density Functional Methods, Part I*; Chong, D., Ed.; World Scientific: Singapore, 1995; pp 155−192.
(37) Casida, M. E. In *Recent Developments and Applications of Modern Density Functional Theory*; Seminario, J., Ed.; Elsevier Science: Amsterdam, 1996; pp 391−439.
(38) López-Lozano, X.; Barron, H.; Mottet, C.; Weissker, H.-C. Aspect-ratio- and Size-dependent Emergence of The Surface-Plasmon Resonance in Gold Nanorods: An Ab Initio TDDFT Study. *Phys. Chem. Chem. Phys.* **2014**, *16*, 1820−1823.
(39) Burke, K.; Perdew, J.; Wang, Y. In *Electronic Density Functional Theory*; Dobson, J., Vignale, G., Das, M., Eds.; Springer: New York, 1998; pp 81−111.
(40) Kresse, G.; Hafner, J. Ab Initio Molecular Dynamics for Liquid Metals. *Phys. Rev. B* **1993**, *47*, 558−561.
(41) Kresse, G.; Furthmüller, J. Efficiency of Ab-Initio Total Energy Calculations for Metals and Semiconductors Using a Plane-Wave Basis Set. *Comput. Mater. Sci.* **1996**, *6*, 15−50.
(42) Kresse, G.; Joubert, D. From Ultrasoft Pseudopotentials to The Projector Augmented-Wave Method. *Phys. Rev. B* **1999**, *59*, 1758−1775.
(43) Pilati, T.; Forni, A. *SYMMOL*: A Program to Find The Maximum Symmetry in An Atom Cluster: An Upgrade. *J. Appl. Crystallogr.* **2000**, *33*, 417.
(44) Negishi, Y.; Sakamoto, C.; Ohyama, T.; Tsukuda, T. Synthesis and The Origin of the Stability of Thiolate-Protected Au_{130} and Au_{187} Clusters. *J. Phys. Chem. Lett.* **2012**, *3*, 1624−1628.
(45) Negishi, Y.; Nakazaki, T.; Malola, S.; Takano, S.; Niihori, Y.; Kurashige, W.; Yamazoe, S.; Tsukuda, T.; Häkkinen, H. A Critical Size for Emergence of Nonbulk Electronic and Geometric Structures in Dodecanethiolate-Protected Au Clusters. *J. Am. Chem. Soc.* **2015**, DOI: 10.1021/ja5109968.

■ NOTE ADDED IN PROOF

After this work had been completed, we learned of the important new and relevant article by Negishi et al.[45] who reported improved optical spectra of the $Au_{144}(SR)_{60}$ as neat-film samples ($R{=}C_{12}H_{25}$) at temperatures as low as 25 K. These impressive new results confirm and extend the prior results, demonstrating the extensive fine spectral structure of this important class of Au144-cluster-based materials. Also, the same article contains new TDDFT calculations of the optical spectra, leading to a substantial revision of the earlier conclusions (by the same subset of co-authors) that the spectra are necessarily devoid of such fine structure, even in the case of the low-symmetry (López-Acevedo et al.[24]) coordinates. These encouraging results lead one to anticipate a greater continuing interest in the resolution of the structural, thermal, and other details underlying the overall agreement as well as the remaining fine discrepancies separating theory and experiment.

DOI: 10.1021/jp512310x
J. Phys. Chem. C 2015, 119, 11250−11259